

## Micro-discharged plasma density, electron temperature and excited xenon density for enhancement of vacuum ultraviolet luminous efficiency in alternating current plasma display panel

**Eun Ha Choi, Philyong Oh, Yoonho Seo and Guangsup Cho**

**Charged Particle Beam and Plasma Laboratory/PDP Research Center, Department of Electrophysics,  
Kwangwoon University, Seoul 139-701, Korea**

**Phone: +82-2-940-5236, E-mail: ehchoi@daisy.kwangwoon.ac.kr**

**Han S. Uhm**

**Department of Molecular Science and Technology, Ajou University, San 5 Wonchon-Dong,  
Paldal-Gu, Suwon 442-749, Korea**

### Abstract

*The plasma ion density in AC-PDP has shown to be increased from  $5.6 \times 10^{11} \text{ cm}^{-3}$  to  $9.0 \times 10^{11} \text{ cm}^{-3}$  as the Xe mixture ratio to neon increase from 1 % to 10 %, respectively, at fixed pressure of 400 Torr, by using the micro-Langmuir probe. It is noted that the plasma ion density is density increases as the gas pressure increases in this experiment. The electron temperature decreases from 2.3 to 1.2 eV as the Xe mole fraction increases from 1 % to 10 % at fixed pressure of 400 Torr, which is measured by the micro Langmuir probe and high-speed ICCD camera in this experiment. It is noted that the electron temperature decreases as the gas pressure increases from 150 to 400 Torr in this experiment. It is also observed that the excited Xe atom density and the plasma ion density are in strong correlation sharp between each other in this experiment. It is noted that  $5.2 \times 10^{12} \text{ cm}^{-3}$  in the  $1s_5$  metastable state and  $1.2 \times 10^{12} \text{ cm}^{-3}$  in the  $1s_4$  resonance state for the PDP cell with gap of 50  $\mu\text{m}$  distances under the fixed gas pressure of 400 Torr and Xe content ratio of 10 %.*

temperature in terms of the xenon mixture ratio to neon and filling gas pressure in AC-PDPs, since the VUV emissions from excited  $\text{Xe}^*$  resonant atoms and molecular dimer  $\text{Xe}_2^*$  in xenon plasma diluted with helium or neon depend upon them [2]. In this context, the space and time resolved light emission from a surface discharged AC-PDP has been investigated using an image intensified charge coupled device (ICCD) camera in order to understand the dynamic characteristics of plasma propagation on the cathode and the anode, as well as the electron temperature and plasma density in AC-PDPs. In the experiment, some of the observed results provide some clues as the origin of the plasma propagation on the sustaining electrodes in AC-PDPs. From previous results of electron temperatures measured by the Langmuir probe [3], [4] and careful examination of propagating distance of the surface-discharged plasma in AC-PDP [1], it is concluded that the plasma propagation speed on the cathode is closely related to the ion acoustic wave [1], [5], [6], which should be initiated within a discharge-current-driven time of 0.2s in a coplanar AC-PDP with a pulse of several tens of kilohertz. The main purpose of this paper is to investigate the electron temperature from its propagation speed of cathode plasma, which is a newly proposed diagnostic methods for measurement of electron temperature in micro discharged plasma, as well as the plasma density from the ion saturation current measured by a Langmuir probe. And also the excited Xe atoms in the  $1s_5$  metastable state and the  $1s_4$  resonance state across the two sustaining electrode have been investigated in

### 1. Introduction

The Surface discharged alternating current plasma display panels (AC-PDPs) utilizes the phenomena of phosphors excited by vacuum ultraviolet (VUV) rays from xenon in the Penning mixture gas. The present AC-PDPs have several problems as low brightness as  $350 \text{ cd/m}^2$  and efficiency as 1.5 lm/W [1]. It is believed that the information on electron temperature and plasma density is one of the major factors in realization of high luminous efficiency from AC-PDPs. Therefore, it is of great importance to investigate the plasma ion density and electron

a micro discharge cell of alternating current plasma display panels by laser absorption spectroscopy method based on the wavelength modulation (WM) technique.

## 2. Experimental Configuration

The panel structure of AC-PDPs with a cell pitch of 1080  $\mu\text{m}$  has been used in the experiment. A sustaining electrode pair, arranged parallel to each other is formed on a glass substrate. The sustaining electrodes are covered by a dielectric layer with a thickness of 30  $\mu\text{m}$ . A MgO protective layer is deposited on the dielectric layer by the electron beam evaporation method with 5000  $\text{\AA}$  in thickness. The electrode gap between the two transparent sustaining electrodes, which is made of indium tin oxide (ITO), is kept at about 50  $\mu\text{m}$  and its width is 300  $\mu\text{m}$ . The bus electrode located on the outer edge of transparent electrodes is made of silver paste and its width is held at 50  $\mu\text{m}$ . For measurement of electron temperature and plasma ion density, the rear glass in AC-PDPs has not been used in this experiment. Inserting a Langmuir probe into the AC-PDP discharge plasma, the current flows into the Langmuir probe because electrons and ions are collected. Using the current-voltage (I-V) characteristic curve obtained by sweeping the probe bias voltage, the diagnostics of electron temperature and plasma density in AC-PDPs can be performed. In this experiment, the ion saturation current together with the high-speed ICCD discharge images have been experimentally measured, and from which the electron temperature and plasma density have been investigated in AC-PDP.

To measure the electron temperature and plasma density in micro-discharged AC-PDPs, the diameter of the probe must be smaller than the sustaining electrode gap.

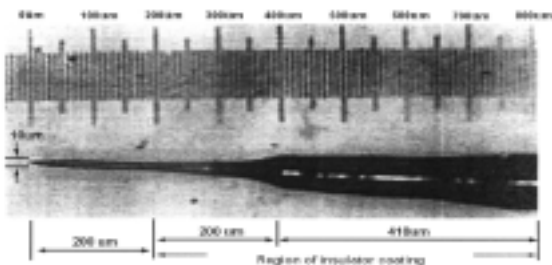


Figure 1. Langmuir Probe tip

Fig. 1 shows the micro-Langmuir probe tip where the diameter is 10  $\mu\text{m}$ , which is manufactured by the electrochemical etching method. The end-edge of 200  $\mu\text{m}$  in the micro probe is not covered with an insulator. Fig. 2 shows the schematic circuit diagram for the Langmuir probe, which is located by 60  $\mu\text{m}$  apart from the front surface of the MgO protective layer.

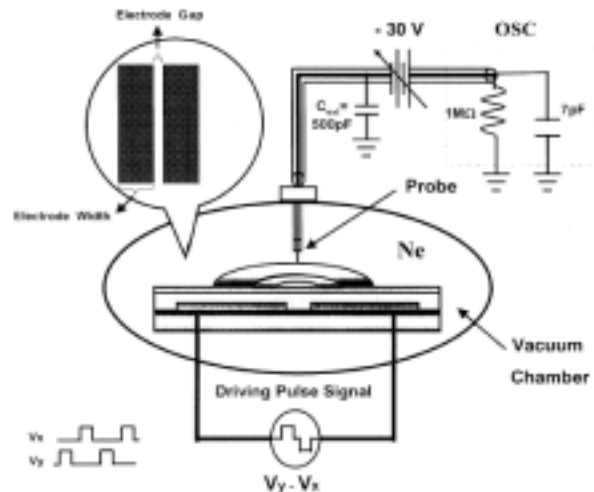
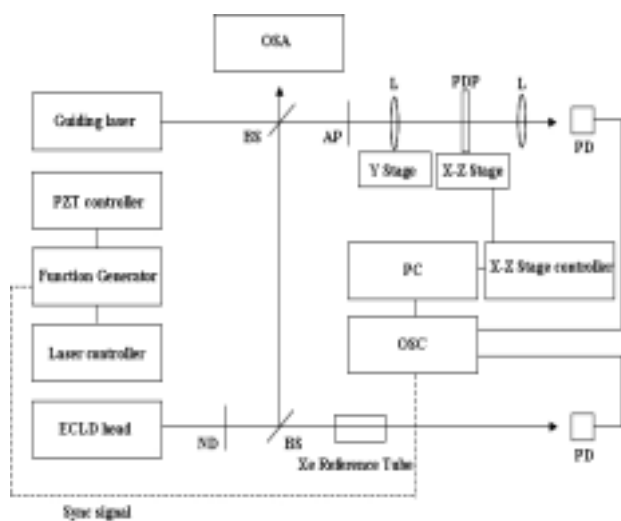


Figure 2. Experimental schematics for the Langmuir probe

In Fig. 2, the sustaining voltages are connected to the sustaining anode and cathode, respectively, for a given moment. They are alternatively changed as time goes by. The probe bias voltage of -30 V has been applied to the micro probe tip for collecting the ion saturation current. The ion saturation current flowing into the Langmuir probe has been obtained by differentiating the oscilloscope output signal of  $Q/C_{\text{ext}}$  where  $Q$  is the charge of ion accumulated on the external capacitance  $C_{\text{ext}} = 500\text{pF}$ . The AC-PDP panel has been operated by the square pulse of the driving frequency 50 kHz with the duty ratio of 40%. The neon gas mixed with xenon mole fraction of 1, 2, 4, 7, and 10 % is used in the present AC-PDP and its pressure is varied from 150 to 400 Torr for a given Xe mole fraction in this experiment. After breakdown, the sustaining voltage is maintained at 270 V. Figure 3 shows experimental schematics of laser absorption spectroscopy [9], [10] used in this experiment. Diode laser system consists of current, temperature, and piezoelectric-transducer (PZT) controllers. The PZT controller is employed for fine tuning of wavelength.



**Figure 3. Experimental schematics for laser absorption spectroscopy**

Also, we make use of Littman type which is tuned by a rotating mirror with high reflectivity along with a fixed diffraction grating in the external cavity. For making fine-frequency adjustments, ramp wave modulation signal with 10 Hz generated from function generator apply for the PZT controller. The laser frequency has been adjusted by an order of -30 GHz to +30 GHz by sweeping the PZT voltage from -3 V to +3 V in this experiment. The diode's output frequency is swept in 0.036 nm per one voltage by the PZT controller. IR Probe beam from the external cavity is splitted into two directions by the first beam splitter. One of which is brought into a Xe reference tube made of external electrode fluorescent tube (EEFL), which is used to monitor the laser's frequency during absorption processes. The EEFL Xe reference tube is filled with pure Xe gas of 0.7 Torr. The EEFL Xe reference tube has advantage of long life time and stabilization of frequency tuning for absorption observation. The other splitted IR laser beam splits again into a PDPs cell through a beam defining aperture by the second beam splitter. The IR probe beam transmitted to a PDPs cell containing Ne-Xe (10%) gas mixtures of 400 Torr has been absorbed by reversed-biased PIN photodiode. The other IR probe beam fed into optical spectrum analyzer (OSA) by the second beam splitter followed by optical fiber collimator for monitoring the laser frequency. For the purpose of guiding IR probe beam, He-Ne laser is led into a PDPs cell along the same IR probe beam path.

Also, to measure laser beam intensity, rear glass with spacer has no addressing electrodes, barrier ribs and phosphors. For preventing saturation from incident IR probe beam into the PDP discharge unit cell, it is attenuated by neutral density filters with OD(optical density) 0.04 to 3.0.

### 3. Experimental Results and Discussions

The electron temperature and plasma density can be measured by  $\Delta \ln I / \Delta V = e/kT$  and  $I_{is} = n_e e A \sqrt{kTe/M}$  from the Langmuir probe, where  $I$  and  $V$  are the probe current and bias voltage, respectively,  $T_e$  is the electron temperature,  $n_e$  is the plasma density. Here,  $A$  is a surface area of the Langmuir probe being taken into account the plasma sheath,  $M$  is the mass of neon ion,  $K$  is the Boltzman constants,  $e$  is the charge of electron, and  $I_{is}$  is the ion saturation current. It is assumed here that the transient slope of  $I$ - $V$  curve from Langmuir probe is not affected by electron collisions with neutrals even though it suffers from collision behaviors with neutrals under high gas pressures. It is also noted that the size of the sheath around the tip of the Langmuir probe is about 3  $\mu\text{m}$ , where in there is no ion collision with neutrals [3], [4]. It is recently observed that the propagation speed of the cathode plasma in AC-PDPs is strongly close to the ion acoustic wave [1], [5], [6], which is given by  $\sqrt{kTe/M}$ . Fig. 4 shows the waveforms of sustaining voltage  $V_{\text{sustain}} = 270\text{V}$  (top), discharge or displacement current (middle), and Langmuir probe signal (bottom) under the probe bias voltage -30 V and the driving frequency of 50 kHz (a) with discharge and (b) without discharge. It is noted that the waveforms of the sustaining voltage and discharge current from plasma of AC-PDPs are not significantly perturbed by the Langmuir probe in this experiment.

It is noted in Fig. 3(a) that the discharge current is occurred within a 0.2 s. The saturation plasma ion current flowed into the Langmuir probe can be obtained by differentiating the probe voltage difference between Fig. 3(a) and (b), which is given by  $I_{is} = C_{ext} (d\Delta V_{probe}) / (dt)$ . With this saturated ion current, the plasma ion density can be obtained by  $n_{is} = I_{is} / eA \sqrt{kTe/M}$ . It is noted that the electron temperature could be obtained either by Langmuir probe [3], [4] or by plasma propagation speed on cathode from high-speed ICCD camera [1].

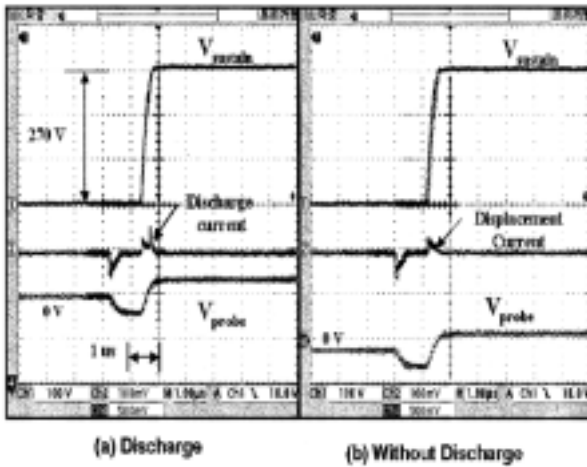


**Figure 4.** Sustaining voltage waveforms (top), discharge or displacement current signals (middle), and Langmuir probe signals (bottom)

It is noted that these electron temperatures from Langmuir probe and ICCD camera are measured to both be about 1.2 eV. Both techniques agree to within 5% of each other.

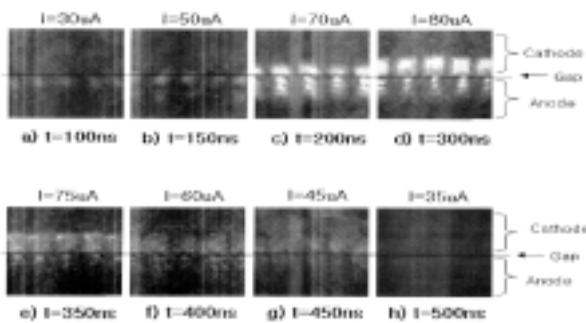


**Figure 5.** High-speed single-frame discharge images taken by ICCD camera.

Fig. 5 shows the high-speed single-frame discharge images taken by ICCD camera at elapsed time from  $t=100$  ns to  $t=500$  ns with respect to the beginning of voltage pulse applied to the cathode and anode electrodes under the gas pressure of 300 torr. The discharge currents corresponding to the Fig. 5 (a) and (d) are 30 and 08  $\mu\text{m}$  per unit cell, respectively. The discharge image in Fig. 4(a)-(d) correspond to the increasing currents of 30 ( $t=100$  ns), 50 ( $t=150$  ns), 70 ( $t=200$  ns), and 80  $\mu\text{A}$  ( $t=300$  ns), which those in Fig 5(e)-(h) correspond to the decreasing ones of 75 ( $t=350$  ns), 60 ( $t=400$  ns), 45 ( $t=450$  ns), and 35  $\mu\text{A}$  ( $t=500$  ns), respectively. It is noted from Fig. 4 that the largest discharge area and brightest light emission

have occurred for the largest current at  $t=300$  ns. The light emission patterns of the anode and cathode are different from each other. It is shown in Fig. 4(a)–(d) that the emission intensity from the cathode is strong and the emission expands outward by ion acoustic wave [1] in time duration between  $t=100$  ns and  $t=300$  ns. On the other hand, emission intensity is weak and the area shrinks inward by the temporal decrease of applied voltage pulse during the time between  $t=300$  ns and  $t=500$  ns. It is noted that striations are observed only on the anode surface. Striations can also be analyzed by an ion wave appearing on the cathode surface [5], [6]. When ions and electrons accumulate separately on the cathode and anode surface in AC-PDPs, ion and electron clouds have self-sustained perturbations to maintain the force balance between them. The perturbed ion density is generated over the cathode surface. These ion bunches on the cathode surface recombine with fast-moving electrons when the polarity of the applied voltage changes. During recombination, the striation fringes are generated with time on the anode surface and gradually expand outward during the time interval  $t=100$  ns and  $t=300$  ns.

The plasma propagation speed on the cathode has been obtained from the  $\Delta x / \Delta t$  in high-speed discharge framing images in Fig. 5, where  $\Delta x$  is the change in propagation distance of cathode plasma between the elapsed time interval  $\Delta t$ . It is noted that the plasma propagation speed on the cathode decreases as the gas pressure increases due to collision effects. The propagation speed of the cathode plasma decreases from 3.0 mm/s to 2.0 mm/s for increasing the gas pressures from 150 to 400 Torr, in this experiment. Fig. 6 shows the ion density and electron temperature as a function of the xenon mixture ratio to neon gas under fixed gas pressure of 400 Torr. The plasma ion density has been measured at the center of the sustaining electrode gap by a micro-Langmuir probe, which is 60  $\mu\text{m}$  away from the MgO front surface of AC-PDPs. It is noted that the plasma ion density has shown to be increased from  $5.6 \times 10^{11} \text{ cm}^{-3}$  to  $9.0 \times 10^{11} \text{ cm}^{-3}$  as Xe mole fraction increases from 1% to 7%, beyond which is saturated at  $9.0 \times 10^{11} \text{ cm}^{-3}$ . It is also noted that the plasma ion density increases as the gas pressure increases in this experiment.

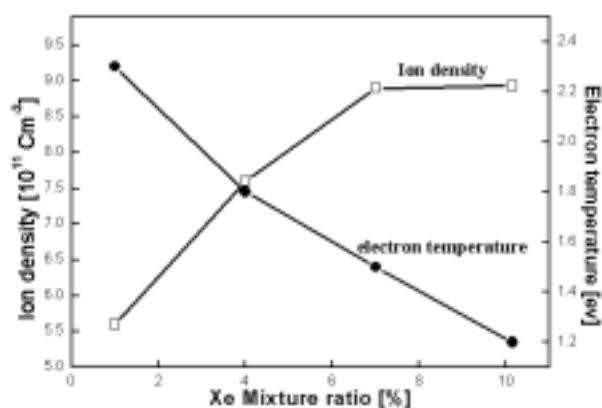


Figure 6. Plasma ion density and electron temperature versus Xe mixture ratio to neon at fixed pressure of 400 Torr.

The electron temperature, in this experiment, has been measured to be 2.3, 2.1, 1.8, 1.5, and 1.2 eV for xenon mole fractions of 1 %, 2%, 4%, 7%, and 10 %, respectively. These measured plasma ion density and electron temperature are shown to be in good agreement with those obtained from laser Thomson scattering method [7]. It is also noted in this experiment that the electron temperature decreases as the gas pressure increases from 150 Torr to 400 Torr. It is noted that the electron-mean-free path might be smaller for the higher gas pressure to result in lower electron temperature and saturated plasma ion density in AC-PDPs [8]. This result shows good agreement with previous study indicating that electron temperature in a high-pressure discharge plasma is proportional to  $E/P$ [8], where  $E$  is electric field and  $P$  is pressure. Figure 7 shows spatial density distribution of excited metastable ( $1S_5$ ), resonance ( $1s_4$ ) xenon and plasma ion density under the sustaining electrode gap 50  $\mu\text{m}$  in coplanar AC-PDPs. Metastable ( $1S_5$ ) and resonance ( $1s_4$ )  $\text{Xe}^*$  density keep on same trend as seen from the Fig. 7. It is also noted that excited xenon density is analogous to tendency of the plasma ion density. The  $\text{Xe}^*$  density and plasma ion density are in strong correlation between each other in this experiment. This result shows that the excited xenon density is proportional to the plasma ion density. It is found that the excited xenon density are maximum to be  $5.2 \times 10^{12} \text{ cm}^{-3}$  in the  $1S_5$  metastable state and  $1.2 \times 10^{12} \text{ cm}^{-3}$  in the  $1s_4$  resonance state, respectively, for the PDP cell with gap of 50  $\mu\text{m}$  distances under the fixed gas pressure of 400 Torr and Xe content ratio of 10 %.

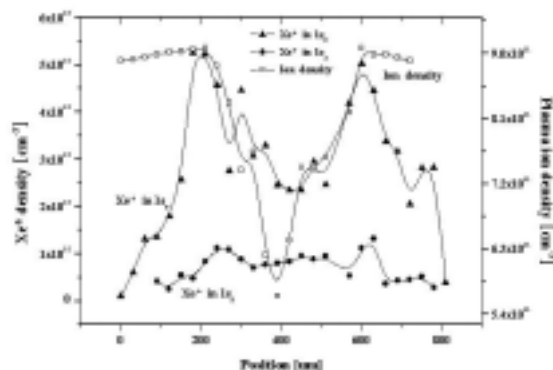


Figure 7. Spatial density distribution of excited Xe atoms in the  $1S_5$ , the  $1s_4$  and plasma ion density

These maximum positions are around at 250  $\mu\text{m}$  away from the center position between the electrodes in a cell. This characteristics might be attributed to the coincidence of the strong electric field line with the discharge ignition path for the maximum wall charges and voltages. It can be seen that there are at least a symmetric peak in spatial distribution of excited xenon density and plasma ion density with respect to the central position for a given sustaining electrode gap. The spatial distribution of excited xenon density correlates with the plasma ion density. These main peaks in spatial distribution of excited xenon density are strongly attributed to the striations appeared on the MgO surface, which are caused by force balance between the accumulated electron and ion charges on the surface in AC-PDP[6].

#### 4. Conclusion

The plasma ion density in AC-PDP has shown to be increased from  $5.6 \times 10^{11} \text{ cm}^{-3}$  to  $9.0 \times 10^{11} \text{ cm}^{-3}$  as the Xe mixture ratio to neon increase from 1 % to 10 %, respectively, at fixed pressure of 400 Torr, by using the micro-Langmuir probe. It is noted that the plasma ion density is density increases as the gas pressure increases in this experiment. The electron temperature decreases from 2.3 to 1.2 eV as the Xe mole fraction increases from 1 % to 10 % at fixed pressure of 400 Torr, which is measured by the micro Langmuir probe and high-speed ICCD camera in this experiment. The driving frequency and height of sustaining voltage are 50 kHz with duty ratio of 40% and 270 V, respectively, in this experiment. It is noted that the

electron-mean-free path might be smaller for the higher Xe mole fraction and gas pressure to result in lower electron temperature and saturated plasma ion density in AC-PDPs, which is in good agreement with the previous theoretical predictions [8]. In this study, it is found that the maximum excited xenon density is  $5.2 \times 10^{12} \text{ cm}^{-3}$  in the  $1s_5$  metastable state and  $1.2 \times 10^{12} \text{ cm}^{-3}$  in the  $1s_4$  resonance state for the PDP cell with gap of 50  $\mu\text{m}$  distances under the fixed gas pressure of 400 Torr and Xe content ratio of 10 %. It is also observed that the excited Xe atom density and the plasma ion density are in strong correlation between each other in this experiment. It is noted that the plasma ion density and excited xenon density are found to be in strong correlation each other for enhancement of VUV efficiency in AC-PDP.

### References

- [1] J. C. Ahn, S. B. Kim, T. S. Cho, M. C. Choi, D. G. Joh, M.W. Moon, Y. Seo, S. O. Kang, G. S. Cho, E. H. Choi, and H. S. Uhm, "Plasma propagation speed and electron temperature in surface discharged alternating current plasma display panels," *Jpn. J. Appl. Phys.*, pt. 1, vol. 41, no. 2A, p. 860, 2002.
- [2] K. Tachibana, S. Feng, and T. Sakai, "Spatiotemporal behaviors of excited Xe atoms in unit discharge cell of ac-type plasma display panel studied by laser spectroscopic microscopy," *J. Appl. Phys.*, vol. 88, p. 4967, 2000.
- [3] J. G. Kim, M. C. Choi, J. C. Ahn, T. S. Cho, D. S. Cho, J. Y. Lim, M. W. Jung, S. H. Choi, S. S. Kim, J. J. Ko, D. I. Kim, C. W. Lee, Y. H. Seo, G. S. Cho, S. O. Kang, and E. H. Choi, "Measurement of electron temperature and plasma density by micro Langmuir probe in alternating current plasma display panels," *Korean Appl. Phys.*, vol. 40, p. 211, 2000.
- [4] J. G. Kim, Y. G. Kim, M. C. Choi, J. C. Ahn, T. S. Cho, D. S. Cho, J. Y. Lim, M. W. Chong, S. H. Choi, J. J. Ko, D. I. Kim, C. W. Lee, Y. H. Seo, G. S. Cho, S. O. Kang, and E. H. Choi, "Measurement of electron temperature and plasma density by micro Langmuir probe in coplanar AC-PDPs," *Int. Display Workshop 99*, p. 675, 1999.
- [5] G. S. Cho, E. H. Choi, Y. G. Kim, H. S. Uhm, Y. D. Joo, J. G. Han, M. C. Kim, and J. D. Kim, "Striations in a coplanar discharge of AC plasma display panels," *J. Appl. Phys.*, vol. 87, p. 4113, 2000.
- [6] G. S. Cho, E. H. Choi, J. G. Kim, Y. G. Kim, J. J. Ko, D. I. Kim, C. W. Lee, Y. H. Seo, and H. S. Uhm, "Analysis of striations in a coplanar discharge," *Jpn. J. Appl. Phys.*, vol. 38, p. 830, 1999.
- [7] Y. Noguchi, A. Matsuoka, K. Uchino, and M. Muraoka, "Direct measurement of electron density and temperature distributions in a micro-discharge plasma for a plasma display panel" *J. Appl. Phys.* 91, p. 613 (2002).
- [8] H. S. Uhm, K. W. Whang, E. H. Choi, and S. S. Kim, "Influence of Penning effects on high-pressure discharge in the plasma display panel," *Phys. Plasmas*, vol. 9, p. 706, 2002.
- [9] K. Tachibana, S. Feng, and T. Sakai, *J. Appl. Phys.*, Vol. 88, No. 9, p.4967, 2000.
- [10] Kunihide Tachibana, Naoki Kosugi and Tetsuo Sakai, *Appl. Phys. Lett.*, Vol. 65, No. 8, P.935, 1994